"Problems of Nonlinear Dynamics and Physics of Condensed Matter"
Collection of Papers dedicated to the 75th birthday
of Professor Leonid I. Manevitch
Moscow, Russia, 2013

NONLINEAR VIBRATIONS AND ENERGY DISTRIBUTION OF CARBON NANOTUBES

Matteo Strozzi[*)], Leonid I. Manevitch[**)], Francesco Pellicano[*)],
Valeri V. Smirnov[**)], Denis S. Shepelev[**)]
[*)]Department of Engineering "Enzo Ferrari", Modena, Italy
matteo.strozzi@unimore.it
[**)]Semenov Institute of Chemical Physics, Moscow, Russia
lmanev@chph.ras.ru

Abstract
The nonlinear vibrations of Single-Walled Carbon Nanotubes are analysed. The Sanders-Koiter elastic shell theory is applied in order to obtain the elastic strain energy and kinetic energy. The carbon nanotube deformation is described in terms of longitudinal, circumferential and radial displacement fields. The theory considers geometric nonlinearities due to large amplitude of vibration. The displacement fields are expanded by means of a double series based on harmonic functions for the circumferential variable and Chebyshev polynomials for the longitudinal variable. The Rayleigh-Ritz method is applied to obtain approximate natural frequencies and mode shapes. Free boundary conditions are considered. In the nonlinear analysis, the three displacement fields are re-expanded by using approximate eigenfunctions. An energy approach based on the Lagrange equations is considered in order to obtain a set of nonlinear ordinary differential equations. The total energy distribution of the shell is studied by considering combinations of different vibration modes. The effect of the conjugate modes participation is analysed.

Key words
Nonlinear vibrations, energy distribution, carbon nanotubes.

1. Introduction

Carbon Nanotubes were discovered in 1991 by Iijima [1], who first analysed the synthesis of molecular carbon structures in the form of fullerenes and reported the preparation of the carbon nanotubes, as helical microtubules of graphitic carbon.

Rao et al. [2] studied the vibrations of SWNTs by Raman scattering experimental techniques with laser excitation wavelengths in the range of the nanometers. They observed Raman peaks, which correspond to vibrational modes of the nanotubes.
Gupta et al. [3] simulated the mechanical behaviour of SWNTs with free edges by using the MD potential. They considered the effect of the chirality and geometry on the natural frequencies of longitudinal, torsional and inextensional modes.
Arghavan and Singh [4] carried out a numerical study on the free and forced vibrations of SWNTs considering the FE method. They studied different boundary conditions, obtaining natural frequencies, mode shapes, time histories and spectra.
Wang et al. [5] examined applicability and limitations of different simplified models of elastic cylindrical shells for general cases of static buckling and free vibrations. They considered Flugge, Donnell thin shell and Donnell shallow shell models.
Strozzi et al. [6] considered the linear vibrations of SWNTs for different boundary conditions in the framework of the Sanders-Koiter thin shell theory. They studied several types of nanotubes by varying aspect ratio and chirality in a wide range of the natural frequency spectrum.
In the present paper, the nonlinear vibrations of SWNTs are analysed. The Sanders-Koiter thin shell theory is applied. The displacement fields are expanded by means of a double series based on harmonic functions for the circumferential variable and Chebyshev polynomials for the longitudinal variable. The Rayleigh-Ritz method is applied to obtain approximate natural frequencies and mode shapes. Free boundary conditions are considered. In the nonlinear analysis, the three displacement fields are re-expanded by using approximate eigenfunctions. The Lagrange equations are then considered in order to obtain a set of nonlinear ordinary differential equations. The total energy distribution is studied by considering different combined modes. The effect of the conjugate modes participation on the energy distribution is analysed.

2. Sanders-Koiter theory

In Figure 1, a circular cylindrical shell having radius R, length L and thickness h is represented; a cylindrical coordinate system (O; x, θ, z) is considered to take advantage from the axial symmetry of the structure, the origin O of the reference system is located at the centre of one end of the cylindrical shell. In Figure 1, three displacement fields are represented: longitudinal u (x, θ, t), circumferential v (x, θ, t) and radial w (x, θ, t), where the radial displacement field w is considered positive outward, (x, θ) are the longitudinal and angular coordinates of an arbitrary point on the middle surface, z is the radial coordinate along the thickness h of the shell and t denotes the time variable. ($\eta = x/L$) is the nondimensional longitudinal coordinate of the shell, ($\beta = h/L$) denotes a nondimensional parameter and τ is the nondimensional time variable, which is obtained by introducing a reference natural frequency ω_0.

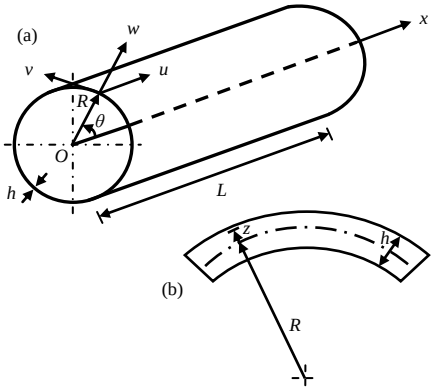

Figure 1. Geometry of the circular cylindrical shell.
(a) Complete shell; (b) cross-section of the shell surface.

2.1. Elastic strain energy

The nondimensional elastic strain energy $\tilde{U}$ of a cylindrical shell, by neglecting the transverse normal stress σ_z (plane stress hypothesis) and the transverse shear strains γ_{xz}, $\gamma_{\theta z}$ (Kirchhoff's hypothesis), is written as

$$\begin{aligned}\tilde{U} = \frac{1}{2}\int_0^1\int_0^{2\pi}\left(\tilde{\varepsilon}_{x,0}^2 + \tilde{\varepsilon}_{\theta,0}^2 + 2\nu\tilde{\varepsilon}_{x,0}\tilde{\varepsilon}_{\theta,0} + \frac{(1-\nu)}{2}\tilde{\gamma}_{x\theta,0}^2\right)d\theta d\eta \\ + \frac{1}{2}\frac{\beta^2}{12}\int_0^1\int_0^{2\pi}\left(\tilde{k}_x^2 + \tilde{k}_\theta^2 + 2\nu\tilde{k}_x\tilde{k}_\theta + \frac{(1-\nu)}{2}\tilde{k}_{x\theta}^2\right)d\theta d\eta\end{aligned} \tag{1}$$

where ($\tilde{\varepsilon}_{x,0}$, $\tilde{\varepsilon}_{\theta,0}$, $\tilde{\gamma}_{x\theta,0}$) are the nondimensional middle surface strains, ($\tilde{k}_x$, $\tilde{k}_\theta$, $\tilde{k}_{x\theta}$) denote the nondimensional middle surface changes in curvature and torsion.

2.2. Kinetic energy

The nondimensional kinetic energy $\tilde{T}$ of a circular cylindrical shell (rotary inertia is neglected) is given by

$$\tilde{T} = \frac{1}{2}\int_0^1\int_0^{2\pi}(\tilde{u}'^2 + \tilde{v}'^2 + \tilde{w}'^2)d\theta d\eta = \frac{1}{2}\int_0^1\int_0^{2\pi}\left[\left(\frac{d\tilde{u}}{d\tau}\right)^2 + \left(\frac{d\tilde{v}}{d\tau}\right)^2 + \left(\frac{d\tilde{w}}{d\tau}\right)^2\right]d\theta d\eta \tag{2}$$

where ($\tilde{u}$, $\tilde{v}$, $\tilde{w}$) are the nondimensional displacement fields, ($\tilde{u}'$, $\tilde{v}'$, $\tilde{w}'$) denote the nondimensional velocity fields.

3. Linear vibration analysis

A modal vibration can be written in the form

$$\tilde{u}(\eta,\theta,\tau)=\tilde{U}(\eta,\theta)\varphi(\tau) \qquad \tilde{v}(\eta,\theta,\tau)=\tilde{V}(\eta,\theta)\varphi(\tau) \qquad \tilde{w}(\eta,\theta,\tau)=\tilde{W}(\eta,\theta)\varphi(\tau) \tag{3}$$

where $\tilde{U}(\eta,\theta)$, $\tilde{V}(\eta,\theta)$, $\tilde{W}(\eta,\theta)$ describe the linear mode shape and $\varphi(\tau)$ denotes the nondimensional time law.

The mode shape is expanded by means of a double mixed series in terms Chebyshev polynomials $T_m^*(\eta)$ in the axial direction and harmonic functions (cos $n\theta$, sin $n\theta$) in the circumferential direction

$$\tilde{U}(\eta,\theta)=\sum_{m=0}^{M_u}\sum_{n=0}^{N}\tilde{U}_{m,n}T_m^*(\eta)\cos n\theta \tag{4}$$

$$\tilde{V}(\eta,\theta)=\sum_{m=0}^{M_v}\sum_{n=0}^{N}\tilde{V}_{m,n}T_m^*(\eta)\sin n\theta \tag{5}$$

$$\tilde{W}(\eta,\theta)=\sum_{m=0}^{M_w}\sum_{n=0}^{N}\tilde{W}_{m,n}T_m^*(\eta)\cos n\theta \tag{6}$$

where $T_m^* = T_m\,(2\eta - 1)$, m is the polynomials degree and n denotes the number of nodal diameters.

3.1. Boundary conditions

Free-free boundary conditions are given by

$$\tilde{N}_x=0 \qquad \tilde{N}_{x\theta}+\tilde{M}_{x\theta}=0 \qquad \tilde{Q}_x+\frac{\partial\tilde{M}_{x\theta}}{\partial\theta}=0 \qquad \tilde{M}_x=0 \qquad \eta=0,1 \tag{7}$$

where the nondimensional force ($\tilde{N}_x, \tilde{N}_{x\theta}, \tilde{Q}_x$) and moment ($\tilde{M}_x, \tilde{M}_{x\theta}$) resultants are expressed in the form

$$\tilde{N}_x=\tilde{\varepsilon}_{x,0}+\nu\tilde{\varepsilon}_{\theta,0} \qquad \tilde{N}_{x\theta}=\frac{(1-\nu)}{2}\tilde{\gamma}_{x\theta,0} \qquad \tilde{M}_x=\frac{\beta^2}{12}(\tilde{k}_x+\nu\tilde{k}_\theta)$$

$$\tilde{M}_{x\theta}=\frac{\beta^2}{12}\frac{(1-\nu)}{2}\tilde{k}_{x\theta} \qquad \tilde{Q}_x=\frac{\beta^2}{12}\left[\tilde{k}_{x,x}+\nu\tilde{k}_{\theta,x}+\frac{(1-\nu)}{2}\tilde{k}_{x\theta,\theta}\right] \tag{8}$$

3.2. Rayleigh-Ritz method

The maximum number of variables needed for describing a general vibration mode with n nodal diameters is obtained by the relation ($N_p = M_u + M_v + M_w + 3 - p$), where ($M_u = M_v = M_w$) denote the degree of the Chebyshev polynomials and p describes the number of equations for the boundary conditions to be respected.

For a multi-mode analysis with different values of nodal diameters n, the number of degrees of freedom of the system is computed by the relation ($N_{max} = N_p \times (N + 1)$), where N represents the maximum value of the nodal diameters n considered.

Equations (3) are inserted into the expressions of the elastic strain energy $\tilde{U}$ (1) and the kinetic energy $\tilde{T}$ (2) to compute the Rayleigh quotient $R(\tilde{\boldsymbol{q}}) = \tilde{U}_{\max} / \tilde{T}^*$, where $\tilde{U}_{\max} = \max(\tilde{U})$ is the maximum of the potential energy during a modal vibration, $\tilde{T}^* = \tilde{T}_{\max} / \omega^2$, $\tilde{T}_{\max} = \max(\tilde{T})$ denotes the maximum of the kinetic energy during a modal vibration, ω represents the circular frequency of the synchronous harmonic motion $\varphi(\tau) = \cos \omega\tau$ and $\tilde{\boldsymbol{q}} = [\ ..., \tilde{U}_{m,n}, \tilde{V}_{m,n}, \tilde{W}_{m,n}, ...\ ]^{\mathrm{T}}$ is a vector containing all the unknown variables built depending on the considered boundary conditions.

After imposing the stationarity to the Rayleigh quotient, one obtains the eigenvalue problem

$$(-\omega^2 \tilde{\boldsymbol{M}} + \tilde{\boldsymbol{K}})\tilde{\boldsymbol{q}} = \boldsymbol{0} \tag{9}$$

which furnishes approximate natural frequencies (eigenvalues) and mode shapes (eigenvectors and eigenfunctions).

The approximate mode shape of the j-th mode is given by the equations (4), (5), (6), where coefficients ($\tilde{U}_{m,n}, \tilde{V}_{m.n}, \tilde{W}_{m,n}$) are substituted with ($\tilde{U}^{(j)}_{m,n}, \tilde{V}^{(j)}_{m,n}, \tilde{W}^{(j)}_{m,n}$), which denote the components of the j-th eigenvector $\tilde{\boldsymbol{q}}_j$ of the equation (9).

The vector function

$$\tilde{\boldsymbol{Q}}^{(j)}(\eta,\theta) = \left[\tilde{U}^{(j)}(\eta,\theta),\ \tilde{V}^{(j)}(\eta,\theta),\ \tilde{W}^{(j)}(\eta,\theta)\right]^T \tag{10}$$

is the approximation of the j-th eigenfunction vector of the original problem.

4. Nonlinear vibration analysis

The displacement fields $\tilde{u}(\eta,\theta,\tau)$, $\tilde{v}(\eta,\theta,\tau)$, $\tilde{w}(\eta,\theta,\tau)$ are expanded by using both the linear mode shapes $\tilde{U}(\eta,\theta)$, $\tilde{V}(\eta,\theta)$, $\tilde{W}(\eta,\theta)$ obtained in the previous linear analysis and the conjugate mode shapes $\tilde{U}_c(\eta,\theta)$, $\tilde{V}_c(\eta,\theta)$, $\tilde{W}_c(\eta,\theta)$ in the form

$$\begin{aligned}
\tilde{u}(\eta,\theta,\tau) &= \sum_{j=1}^{N_u}\sum_{n=1}^{N}\left[\tilde{U}^{(j,n)}(\eta,\theta)\varphi_{u,j,n}(\tau)+\tilde{U}_c^{(j,n)}(\eta,\theta)\varphi_{u,j,n,c}(\tau)\right] \\
\tilde{v}(\eta,\theta,\tau) &= \sum_{j=1}^{N_v}\sum_{n=1}^{N}\left[\tilde{V}^{(j,n)}(\eta,\theta)\varphi_{v,j,n}(\tau)+\tilde{V}_c^{(j,n)}(\eta,\theta)\varphi_{v,j,n,c}(\tau)\right] \\
\tilde{w}(\eta,\theta,\tau) &= \sum_{j=1}^{N_w}\sum_{n=1}^{N}\left[\tilde{W}^{(j,n)}(\eta,\theta)\varphi_{w,j,n}(\tau)+\tilde{W}_c^{(j,n)}(\eta,\theta)\varphi_{w,j,n,c}(\tau)\right]
\end{aligned} \tag{11}$$

The Lagrange equations of motion for free vibrations are expressed in the form

$$\frac{d}{d\tau}\left(\frac{\partial\tilde{L}}{\partial\dot{\tilde{q}}_i}\right)-\frac{\partial\tilde{L}}{\partial\tilde{q}_i}=0 \qquad i\in[1,N_{\max}] \qquad (\tilde{L}=\tilde{T}-\tilde{U}) \tag{12}$$

Using the Lagrange equations (12), a set of nonlinear ordinary differential equations is obtained; such system is then solved by using numerical methods.

5. Numerical results

In order to analyse the discrete carbon nanotube as a continuum shell, equivalent parameters must be considered [5]. These parameters are independent from the CNT diameter (no size effect). The nanotube of Table 1 is used for the computations.

Effective thickness h_0 (nm)	0.10 ÷ 0.15
Equivalent thickness h (nm)	0.066
Effective Young's modulus E_0 (TPa)	1.0 ÷ 2.0
Equivalent Young's modulus E (TPa)	5.5
Effective Poisson's ratio v_0	0.12 ÷ 0.28
Equivalent Poisson's ratio v	0.19
Surface density of graphite σ (kg/m^2)	7.718×10^{-7}
Equivalent mass density ρ (kg/m^3)	11700

Table 1. Effective and equivalent parameters of the Single-Walled Carbon Nanotube [5].

The present model is validated with the molecular dynamics data available in the literature [3]; the results reported in Table 2 show that the present model is accurate.

Natural frequency (THz)			Difference %
(r, s)	SKT - Present model	MDS - Ref. [3]	
(10, 0)	8.966	8.718	2.84
(6, 6)	8.636	8.348	3.45
(12, 0)	7.478	7.272	2.83
(7, 7)	7.399	7.166	3.25
(8, 8)	6.473	6.275	3.15
(14, 0)	6.414	6.235	2.87
(16, 0)	5.606	5.455	2.77
(10, 10)	5.184	5.026	3.14

Table 2. Natural frequencies of the radial breathing mode (j = 0, n = 0): comparisons between the Sanders-Koiter theory (SKT) and the Molecular Dynamics Simulations (MDS).

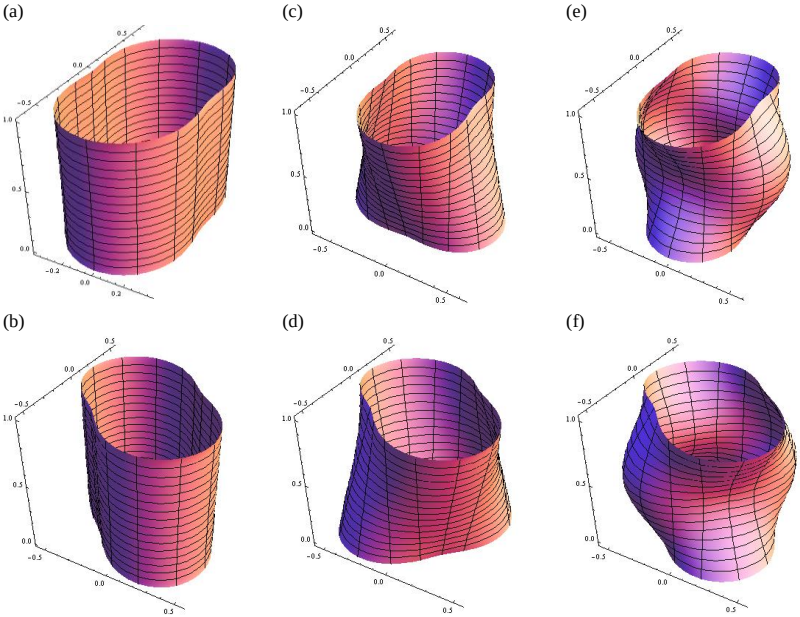

Figure 2. Mode shapes of the SWNT (r = 10, s = 0, L = 10 nm). Equivalent parameters. Free edges. (a),(b) Conjugate modes (0,2); $f_{0,2}$ = 1.17609 THz. (c),(d) Conjugate modes (1,2); $f_{1,2}$ = 1.21558 THz. (e),(f) Conjugate modes (2,2); $f_{2,2}$ = 1.52195 THz.

In Figures 2(a-f), three mode shapes of a free-free carbon nanotube are presented, such modes are considered for the development of the semi-analytic nonlinear model of the carbon nanotube in the re-expansion of Equation (11).

In Figures 3-8, time histories and energy distributions in linear and nonlinear field are represented. Different modes are studied. The carbon nanotube is unwrapped on a plane to allow the energy representation. The damping is not considered and the total energy is constant (integral of the density over the surface).

In Figures 3(a-b), the time histories of the combined modes (0,2), (2,2) in linear field are presented. Different initial conditions on the two combined modes are imposed: mode (0,2), thick line, is activated by an initial energy double compared with mode (2,2), thin line, as shown in Figure 3(a). In Figure 3(b), enlarged view of Figure 3(a), the time history corresponding to a whole time period of the mode (0,2) is reported, which is different from the time period of the mode (2,2).

The sequence of Figures 4(a-f) shows the distribution of the energy density [Jm^{-2}] in linear field for the combined modes (0,2), (2,2) in the time range corresponding to Figure 3(b). The analysis of the total energy distribution over the shell surface shows a periodicity along the circumferential direction. Moreover, the energy is distributed symmetrically with respect to the longitudinal direction because symmetric modes (0,2) and (2,2) are combined.

In Figures 5(a-b), the time histories of the combined modes (0,2), (2,2) in nonlinear field are presented. The same initial conditions on the combined modes of the linear case are imposed, Figure 5(a). In Figure 5(b), enlarged view of Figure 5(a), the time history corresponding to a whole time period of the first mode is reported, which is different to the time period of the second mode.

Figures 6(a-f) show the distribution of the energy density in nonlinear field for the combined modes (0,2) and (2,2) in the time range corresponding to Figure 5(b). By comparing the linear and nonlinear analyses (with the same initial conditions), we obtain that the nonlinear distribution evolves in a more complex patter, where the total energy periodicity and symmetry are preserved along the circumferential and longitudinal direction, respectively.

In Figures 7(a-b), the time histories of the two conjugate modes (1,2) in nonlinear field are presented. The initial conditions on the conjugate modes are different: the first one, thick line, is activated while the second one, thin line, is slightly perturbed, i.e., an infinitesimal initial energy is provided. After a suitably long time period, as shown in Figure 7(a), the conjugate mode having an infinitesimal initial energy is activated, and it vibrates with large amplitude: this is caused by an energy transfer probably due to an internal resonance (1:1). In Figure 7(b), enlarged view of Figure 7(a), the time history corresponding to a whole time period of the first conjugate mode is reported, which is twice the time period of the second conjugate mode.

The sequence of Figures 8(a-f) shows the energy density distribution in nonlinear field for the two conjugate modes (1,2) in the time range corresponding to Figure

7(b). The periodicity along the circumferential direction is preserved. The activation of the second mode implies an energy transfer between the two conjugate modes. The participation of both the conjugate modes gives rise to a travelling wave moving circumferentially around the shell.

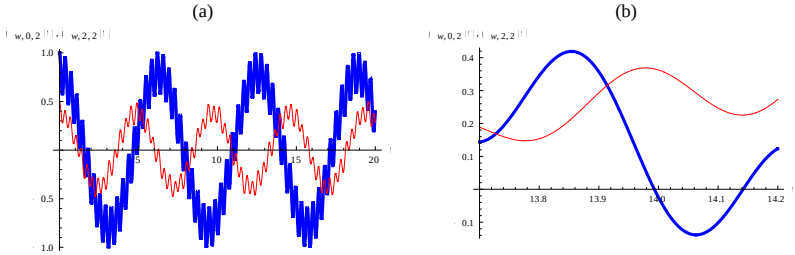

Figure 3. Time histories of the combined modes (0,2), (2,2). Linear analysis. Radial modal coordinates $\varphi_{w,j,n}(\tau)$. Nondimensional time τ. "—", mode (0,2); "—", mode (2,2).

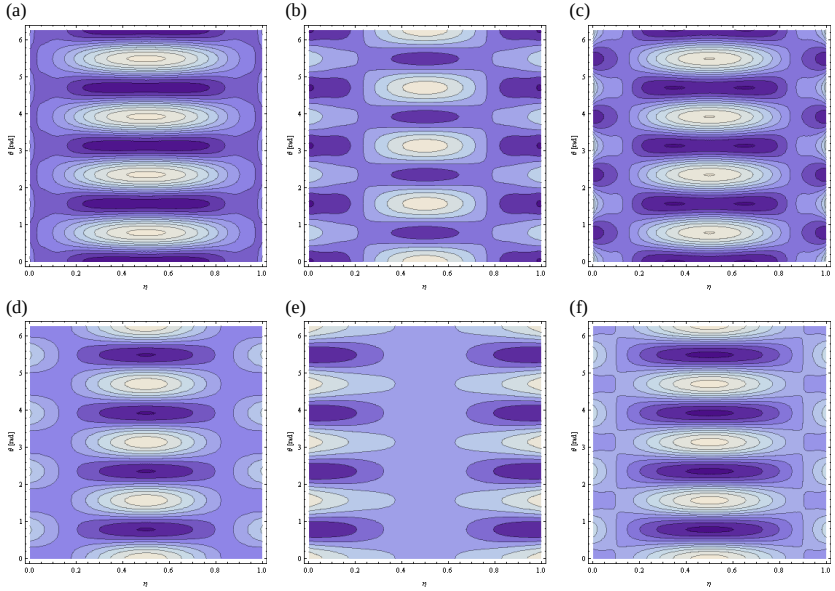

Figure 4. Total energy distribution $\tilde{E}(\eta, \theta, \tau)$. Combined modes (0,2), (2,2). Linear analysis. (a) τ = 13.76. (b) τ = 13.82. (c) τ = 13.94. (d) τ = 14.00. (e) τ = 14.08. (f) τ = 14.20.

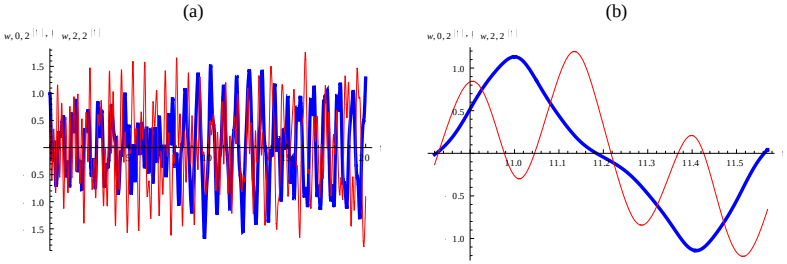

Figure 5. Time histories of the combined modes (0,2), (2,2). Nonlinear analysis. Radial modal coordinates $\varphi_{w,j,n}(\tau)$. Nondimensional time τ. "—", mode (0,2); "—", mode (2,2).

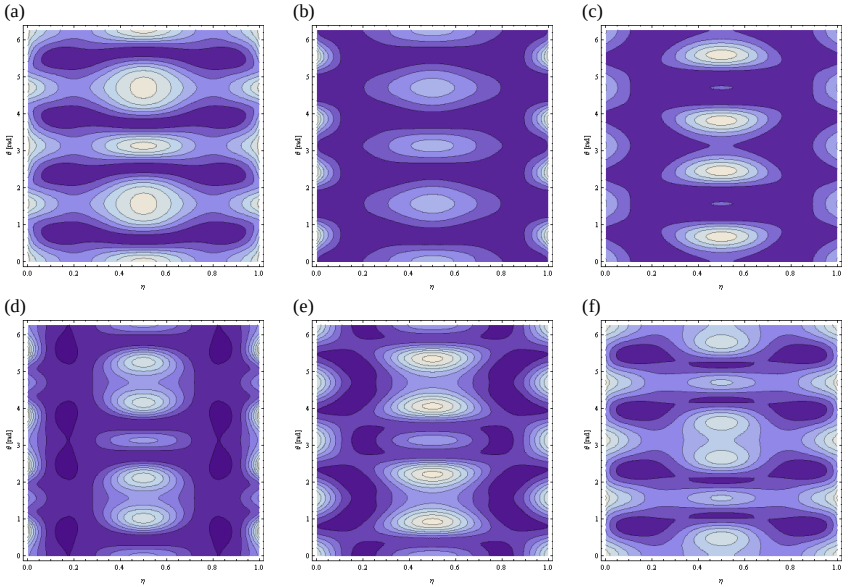

Figure 6. Total energy distribution $\tilde{E}(\eta, \theta, \tau)$. Combined modes (0,2), (2,2). Nonlinear analysis. (a) τ = 10.88. (b) τ = 10.91. (c) τ = 11.00. (d) τ = 11.15. (e) τ = 11.39. (f) τ = 11.54.

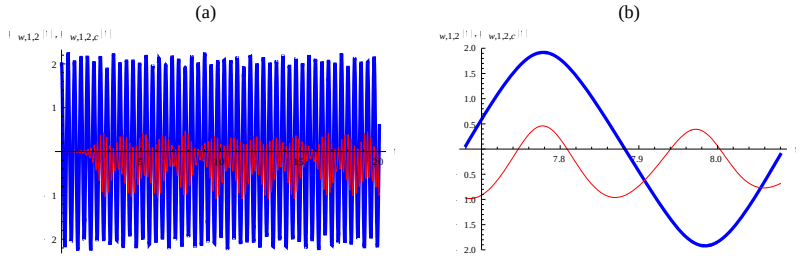

Figure 7. Time histories of the two conjugate modes (1,2). Nonlinear analysis. Radial modal coordinates $\varphi_{w,j,n}(\tau)$. Nondimensional time τ. "—", mode (1,2); "—", mode (1,2,c). (a) Transient included. Energy transfer. (b) Steady state. Time period of the first mode.

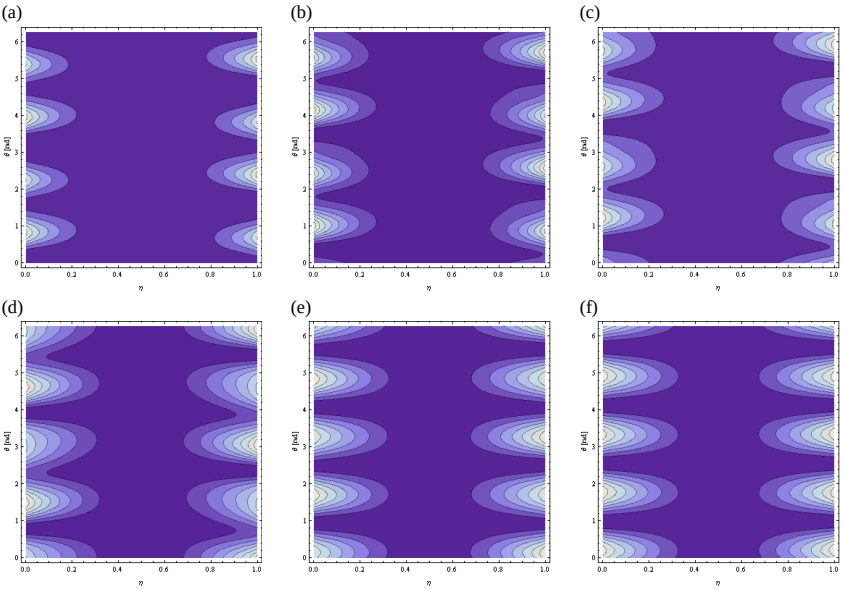

Figure 8. Total energy distribution $\tilde{E}(\eta, \theta, \tau)$. Conjugate modes (1,2). Nonlinear analysis. (a) $\tau = 8.00$. (b) $\tau = 8.02$. (c) $\tau = 8.04$. (d) $\tau = 8.06$. (e) $\tau = 8.08$. (f) $\tau = 8.10$.

6. Conclusions

The nonlinear vibrations of SWNTs are studied within the framework of the Sanders-Koiter elastic shell theory. The Rayleigh-Ritz method is applied in order to obtain approximate natural frequencies and mode shapes. The present model is validated in linear field with data available in the literature. An energy approach based on the Lagrange equations is considered to obtain a set of nonlinear ordinary differential equations. The total energy distribution is analysed in linear and nonlinear fields by assuming suitable initial conditions. The nonlinear energy distribution evolves in a complex pattern with periodicity along the circumferential direction. The participation of two conjugate modes gives rise to an energy transfer between the modes. The periodicity along the circumferential direction is preserved. A travelling wave moving circumferentially around the shell takes place.

7. References

1. Iijima S. (1991) Helical microtubules of graphitic carbon. Nature, 354, 56–58.

2. Rao A.M., Richter E., Bandow S., Chase B., Eklund P.C., Williams K.A., Fang S., Subbaswamy K., Menon M., Thess A., Smalley R.E., Dresselhaus G., Dresselhaus M.S. (1997) Diameter-Selective Raman Scattering from Vibrational Modes in Carbon Nanotubes. Science, 275, 187–191.

3. Gupta S.S., Bosco F.G., Batra R.C. (2011) Wall thickness and elastic moduli of single-walled carbon nanotubes from frequencies of axial, torsional and inextensional modes of vibration. Computational Materials Science, 47, 1049–1059.

4. Arghavan S., Singh A.V. (2011) On the vibrations of single-walled carbon nanotubes. Journal of Sound and Vibration, 330, 3102–3122.

5. Wang C.Y., Ru C.Q., Mioduchowski A. (2004) Applicability and Limitations of Simplified Elastic Shell Equations for Carbon Nanotubes. Journal of Applied Mechanics, 71, 622–631.

6. Strozzi M., Manevitch L.I., Pellicano F., Smirnov V.V., Shepelev D.S. Low-frequency linear vibrations of Single-Walled Carbon Nanotubes: analytical and numerical models. Journal of Sound and Vibration (in press).